PHYSICAL REVIEW B **83**, 115329 (2011)

Diffusion and interface growth in hafnium oxide and silicate ultrathin films on Si(001)

L.V. Goncharova,[1,*] M. Dalponte,[1] T. Feng,[1] T. Gustafsson,[1] E. Garfunkel,[2] P.S. Lysaght,[3] and G. Bersuker[3]
[1]*Departments of Physics and Astronomy, Rutgers University, 136 Frelinghuysen Road, Piscataway, New Jersey 08854, USA*
[2]*Department of Chemistry and Chemical Biology, Rutgers University, 136 Frelinghuysen Road, Piscataway, New Jersey 08854, USA*
[3]*Sematech, Austin, Texas 78741, USA*

(Received 30 November 2010; revised manuscript received 24 January 2011; published 25 March 2011)

Medium energy ion scattering has been used in combination with ^{16}O and ^{18}O isotope tracing to determine elemental depth distributions and elucidate oxygen transport in 2–5 nm thick HfO_2 and $HfSiO_x$ films grown by atomic layer deposition on Si(001). Both the oxygen isotope exchange rate in the dielectric as well as the interfacial silicon oxide growth rates were examined as a function of time, temperature, film stoichiometry (HfO_2, $HfSiO_x$, and $HfSiO_xN_y$), and crystallinity. The amount of exchanged oxygen in the oxide was found to decrease with increasing SiO_2 content. When the SiO_2 to HfO_2 ratio reaches 1:1 in $HfSiO_x$ an almost full suppression of the oxygen exchange is observed. The activation barrier for the SiO_2 growth at the HfO_2/Si and $HfSiO_x$/Si interfaces was found to be much lower than that in the SiO_2/Si and SiO_xN_y/Si cases, which is attributed to distinctly different oxygen incorporation mechanisms. The primary route for oxygen delivery to the interface responsible for the SiO_2 growth is via exchange, however, direct oxidation by molecular oxygen cannot be discounted completely. In the presence of an interfacial nitride layer the ^{18}O-^{16}O exchange is replaced by the ^{18}O-N exchange, which slows diffusion and reduces the oxidation rate.

DOI: 10.1103/PhysRevB.83.115329 PACS number(s): 68.35.Dv, 68.35.Fx, 68.35.Ct, 68.49.Sf

I. INTRODUCTION

The continued scaling of microelectronic components has made the introduction of new materials in complementary metal–oxide–semiconductor (CMOS) technology necessary.[1,2] Transition metal (Hf, Zr, La) oxides, silicates, and ternary Hf-based oxides with a dielectric constant higher than that of SiO_2 are being widely investigated as a dielectric for gate stack and other applications[3,4] and devices based on such materials are now commercially available from some manufacturers. These new metal-oxide-based materials often have poor electrical performance (i.e., instability of the threshold potential – V_T)[5,6] believed to be connected to the presence of a large number of Si dangling bonds, traps, and other defects at or near the dielectric/Si interface. To minimize such interface defects and optimize the electrical characteristics, it has been found to be desirable to have at least one monolayer of SiO_2 at the dielectric/Si interface. The Hf oxide (silicate)/Si interface region is strongly affected by the surface preparation prior to dielectric growth,[7] by growth chemistry, thermal treatment, and, often, also by the nature of the metal gate.[8–10] There is a large body of work that addresses issues pertaining to interface preparation and characterization.[7,8,11–13]

Although SiO_2 films are thermodynamically stable on Si, some higher-κ oxides are not.[1,3,14] Additional complications arise from the fact that the overlayer metal-oxygen ratio may not be perfectly stoichiometric during growth. The deposition of high-κ oxides on silicon are often accompanied by the growth of an interfacial SiO_2 layer, as well as interdiffusion and/or chemical reactions between the overlayers.[15] As a rule, the high-κ dielectric stacks require a postdeposition anneal to passivate defects that contribute to current leakage and threshold voltage instability. The anneal ambient may either intentionally be oxygen rich or contain traces of oxygen as in the case of N_2. Therefore understanding the process of oxygen incorporation during postdeposition processing of high-κ gate stacks is of critical importance for meeting device performance specifications.

In contrast to SiO_2, hafnium oxides and silicates interact strongly with diffusing oxygen, even at relatively low temperatures. The exchange[16] of oxygen from the gas phase with oxygen atoms in the film (which we monitor using oxygen isotopes) occurs throughout the bulk of the high-κ film. On the atomic level the fundamental mechanism of O diffusion in ultrathin (∼10–30 Å) hafnium oxide and hafnium silicate layers remains under debate, in particular, defining the relative role of oxygen vacancies,[17] interstitial oxygen, molecular vs atomic vs ionic species, grain boundaries, and other modes of transport. Defects in the high-κ dielectric layer cannot only impact O transport, but they also negatively impact device performance. First-principles calculations show that the most prominent point defects in monoclinic HfO_2 are positively charged O and negatively charged Hf vacancies.[18] However, oxygen interstitials are more important than oxygen vacancies for diffusion processes as the former have a smaller migration barrier.[19] The amorphous HfO_2 phase has been investigated recently using *ab initio* computational methods to compare the formation and migration of O vacancy, O interstitial, and Hf vacancy point defects in various charge states.[20,21] The lowest migration barrier was predicted for the positively charged O vacancy. In practice, both amorphous and crystalline phase behavior are important since even initially amorphous-grown thin dielectric films are thought to crystallize (Hf oxide)[22] or perhaps even phase separate (Hf silicate)[23] at temperatures comparable with typical processing steps.

If molecular oxygen can diffuse directly to the interface (as it does in SiO_2/Si, perhaps in HfO_2 via defects or voids) then the oxidation reaction could take place right at the semiconductor interface without reacting with the high-κ dielectric.

When oxygen arrives at the lower interface region (regardless of the transport mechanism) it reacts with Si or SiO_{2-x} forming SiO_2. Additional side reactions are also to be expected (e.g., oxygen arrival to the high-κ/Si interface may trigger the injection of Si interstitials from the substrate due to the more open structure in SiO_2 relative to Si[24]). These interstitials can react with oxygen in the SiO_2 overlayer forming SiO locally which can be removed from the film as observed in ^{29}Si isotopic tracing experiments,[25] or can be transported into the high-κ film, changing its composition.

In this paper we experimentally investigate diffusion and exchange reactions and growth interface in ultrathin Hf oxide and silicate films on Si(001). In particular, using high-resolution ion scattering, we have examined a series of different dielectric structures (HfO_2, $HfSiO_x$, and $HfSiO_xN_y$)/Si(001) before and after crystallization annealing, and specifically looked at diffusion of oxygen in these 2–3-nm thick films using isotopic tracing. Oxygen exchange and incorporation rates were studied as a function of oxidation time, temperature, film composition (amount of silica in dielectric), crystallinity, and the presence of nitrogen at the interface. We compare our results for the silicon oxide growth rate in $Hf_xSi_{1-x}O_2$/Si with that of growth at the interface of pure 4–5 nm SiO_2/Si and SiO_xN_y/Si(001) studied earlier.[26–28]

II. EXPERIMENTAL

Hf oxide and silicate films 2–3-nm thick were deposited on a 1 nm SiO_2/Si(001) or 1 nm SiO_xN_y/Si(001) film using atomic layer deposition (ALD) at 600 K with O_3 as an oxidation agent.[29] The stoichiometry of $Hf_{1-x}Si_xO_2$ ($x = 0, 0.33, 0.67$) was controlled by adjusting the relative amounts of hafnia and silica precursors. Nitrogen was introduced into selected samples by postgrowth anneal in NH_3 (973 K, 60 s). As a result a 5:1 = O:N ratio was achieved. To understand the suppression of the O exchange in Hf silicates, we deposited a ~2 ML thick SiO_2 layer on top of an HfO_2 film. Postgrowth oxidation in $^{18}O_2$ (98% isotopically enriched) was performed *in situ* in the UHV chamber ($p_{\text{base}} \sim 10^{-9}$ Torr) connected to the medium energy ion scattering (MEIS) analysis chamber. The sample was first stabilized at a temperature in the ~763–1223 K range (measured by an optical pyrometer and or a *K*-type thermocouple), followed by $^{18}O_2$ or $^{16}O_2$ gas introduction at a pressure of 0.01 Torr (5–30 min).

Medium energy ion scattering was used to determine the depth profile of all elements in the dielectric layers. We used an H^+ beam with the incident beam normal to the surface. A toroidal electrostatic energy analyzer detector[30] was used centered at a scattering angle of 125.27^o corresponding to a high symmetry direction in the substrate. An incident ion energy of 130.8 keV energy was chosen to resolve the ^{18}O and ^{16}O peaks,[31] which is close to the maximum stopping power for protons in Si. Depth profiles of all elements were obtained using a computer simulation code of the backscattered ion energy distributions developed by Nishimura.[32] The depth resolution is estimated to be ~3 Å at the surface and ~8 Å at a depth of 30 Å (Ref. 33).

Si, ^{18}O, and ^{16}O peaks for all samples were carefully examined to quantitatively determine the depth distribution of both oxygen species and Si throughout the dielectric film. Rates of the silicon oxide growth at the Hf dielectric/Si(001) were analyzed, and factors affecting oxygen exchange[26] such as film composition and phase separation were examined.

Complementary x-ray photoemission spectroscopy (XPS) and atomic force microscopy (AFM) measurements were conducted *ex situ*. A commercial XPS system (PHI 5000 series ESCA spectrometer, Al/Mg dual anode source, concentric hemispherical analyzer) was used with a photoelectron take-off angle of 45° and using Al Kα radiation (1486.6 eV). The instrument was calibrated with the Au $4f_{7/2}$ level at 83.9 eV. Charging, when present, was corrected by referencing the energy scale to the C1*s* peak to 285 eV. AFM images were taken under ambient conditions in the "tapping" mode using 125 μm long silicon cantilevers with resonant frequencies ~250 kHz.

III. RESULTS

Figure 1 shows an H^+ backscattered energy spectrum from an as-deposited $Hf_{0.67}Si_{0.33}O_2/SiO_xN_y$/Si(001) film. The proton energies corresponding to the high-energy edges of the Hf, Si, O, and C (but not N) peaks are in excellent agreement with binary collision model calculations, which means that all these elements can be found at the surface, while the nitrogen is buried. The intensity distribution of Si indicates a concentration variation with depth with a Si peak maximum occurring at an energy corresponding to a depth well below the surface. A simulation of this spectrum showed that the outermost layer of this sample was a stoichiometric $Hf_{0.67}Si_{0.33}O_2$ film with a thickness of 27 ± 2 Å. Again, the position of the N peak indicates that there is no N diffusion to the vacuum/$Hf_{0.67}Si_{0.33}O_2$ interface, and all nitrogen is confined within the interfacial SiO_xN_y layer, while the width of the oxygen peak has contributions from both the Hf silicate and the interfacial layer. A small amount of hydrocarbon contamination at the top surface is apparent from a minor C surface peak.

MEIS data represent averages over a sample area of about 0.1 mm^2, making it difficult to distinguish between near interface compositional gradients and interface or surface roughness. Therefore we performed controlled atomic-

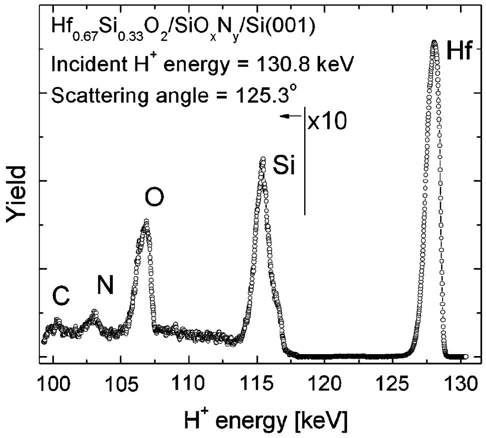

FIG. 1. Backscattering spectrum for as-deposited $Hf_{0.67}Si_{0.33}O_2/SiO_xN_y$/Si(001) film in the channeling alignment.

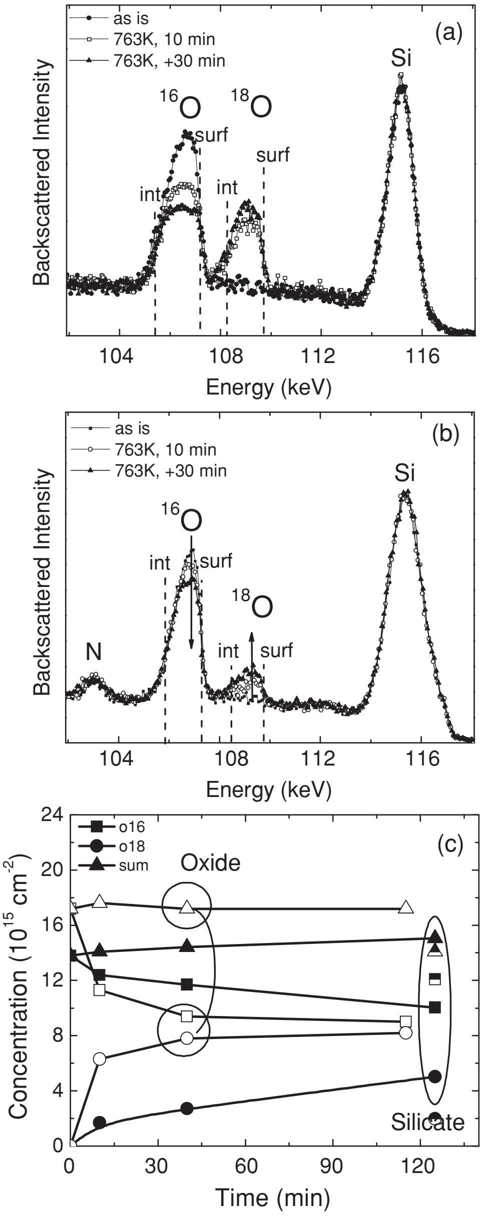

FIG. 2. Variation of ^{18}O and ^{16}O peaks for (a) the $HfO_2/SiO_2/Si$(001) and (b) the $Hf_{0.67}Si_{0.33}O_2/SiO_xN_y/Si$(001) films as a function of re-oxidation time. (c) Oxygen exchange kinetics curves in hafnium oxide (open symbols) and hafnium silicate (dark symbols) films.

force microscopy measurements for selected as-deposited and annealed samples, which revealed rms values of ~2 Å for as-deposited and less than 5 Å for the annealed films.[9]

To investigate the mobility of oxygen, samples were reoxidized in $^{18}O_2$ (after having been annealed briefly at 523–573 K to remove surface carbon). Postdeposition anneals in $^{18}O_2$ were performed at various temperatures, times, and film compositions. Our initial findings indicated that at ~773 K interactions between the high-κ film and oxygen were limited to exchange reactions [i.e., there is no net increase in oxygen ($^{16}O + {}^{18}O$) areal densities, therefore no additional SiO_2 formation].

A. Exchange reactions

Figure 2(a) shows the part of the backscattered H^+ spectrum corresponding to the two oxygen isotopes in $HfO_2/SiO_2/Si$(001) films as reoxidation proceeds. A pronounced ^{18}O peak (spanning from the outer surface of HfO_2 to the SiO_2 interfacial layer, as illustrated by the matched ^{16}O and ^{18}O peak base energy range) is observed after 10 min of $^{18}O_2$ exposure ($p_{18O2} = 0.01$ Torr, 763 K). Concurrent with the development of the ^{18}O peak, the intensity of the ^{16}O peak decreases. This observation shows that the ^{18}O peak is likely not due to $^{18}O_2$ molecular diffusion through the hafnium oxide to the Si interface (as in SiO_2/Si), but rather due to an exchange reaction in the high-κ film (i.e., ^{16}O leaves the surface and ^{18}O goes into the high-κ film).[29] After a longer (40 min) $^{18}O_2$ exposure there is a larger increase in the ^{18}O aerial density and decrease in the ^{16}O density, however, the total oxygen content (sum of ^{16}O and ^{18}O), as calculated from the oxygen peak area, remains the same. (Note that for the same ^{18}O and ^{16}O content and distribution, the ^{18}O peak should have a $(^{18}/_{16})^2 \sim 1.27$ higher intensity than the ^{16}O peak because of the different scattering cross sections.) Based on a full analysis of the Hf, Si, and O peak shapes and energies, we conclude that this as-deposited HfO_2 film has a slight excess of oxygen compared to the ideal 1:2 stoichiometry, and a 6–7 Å interfacial SiO_2 layer. Using transmission infrared spectroscopy, we could also easily detect SiO_2 (not shown).

$Hf_{0.67}Si_{0.33}O_2/SiO_xN_y/Si$(001) films behave slightly dissimilarly. Under the same processing conditions $Hf_{0.67}Si_{0.33}O_2/SiO_xN_y/Si$(001) films [Fig. 2(b)] show a noticeably lower O exchange fraction compared to the $HfO_2/SiO_2/Si$(001) films in Fig. 2(a). There are no changes in the N, Si, and Hf peaks (not shown) for both the Hf oxide and the silicate films, implying that there is no additional interfacial SiO_2 growth (at these temperatures) and that atomic O diffusion through the interfacial SiO_2 ($Si_3N_{4-n}O_n$) layer is inefficient under these experimental conditions.

The concentrations of both oxygen isotopes as a function of the $^{18}O_2$ exposure time are shown Fig. 2(c). The exchange rate in Hf oxide films (open cycles) was, as mentioned above, faster than for Hf silicates. The oxygen exchange fraction reaches >90% of its final value in 10 min for HfO_2, whereas for Hf silicates the exchange is much slower and continues, at the listed experimental conditions, even after 120 min. We believe the saturation of exchange for the Hf oxide is governed by the onset of the crystallization as discussed below.

To quantify and compare the amount of ^{18}O incorporated into the high-κ layer, we estimate the ^{18}O exchange fraction f as the ratio of ^{18}O to the total oxygen ($^{16}O + {}^{18}O$) MEIS areal density in an $Hf_{1-x}Si_xO_{2-n}N_n$ films (excluding any interfacial SiO_2). Table I summarizes representative exchange fractions for selected as-deposited and crystalline Hf oxide, silicate, and silica oxynitride films. Notably, the oxygen exchange fraction for recrystallized oxides and silicate films are lower than for the as-deposited film. Since the annealing temperature may be sufficient to induce chemical phase separation in this composition of the Hf silicate, the lower O exchange fraction observed likely results from a lower surface area of HfO_2 exposed to oxygen, or a suppression of the diffusion through the silica-enriched grain boundaries regions. It is interesting

TABLE I. Areal densities of different oxygen isotopes before and after annealing in $^{18}O_2$ atmosphere ($p_{18O2} = 10^{-2}$ Torr) at 490°C for 30 min.

Composition	Total oxygen ($\times 10^{15}$ atoms/cm^2)	^{16}O loss (^{18}O gain) ($\times 10^{15}$ atoms/cm^2)	Exchange fraction f
HfO_2	15.6	7.8 (7.8)	0.50
HfO_2 (crystalline)	14.7	5.6 (5.8)	0.40
$Hf_{0.67}Si_{0.33}O_2$	13.3	2.6 (2.6)	0.20
$Hf_{0.33}Si_{0.67}O_2$	14	<0.5 (0.5)	<0.04
SiO_2/HfO_2	19.5	1.0 (1.0)	0.07
$Hf_{0.67}Si_{0.33}O_{1.67}N_{0.33}$	11.0	2.1 (2.1)	0.20

to mention that nitrogen incorporation in the Hf silicates does not change the exchange fraction significantly.

B. Interfacial silicon oxide growth

For all thin films, as annealing temperatures increase above 763 K, interfacial silicon oxide growth is observed in addition to the exchange in the Hf dielectric layer. Figures 2(a) and 2(b) show no net increase in interfacial silicon oxide. The evolution of the Si and O ion scattering peaks for $Hf_{0.67}Si_{0.33}O_2/SiO_xN_y/Si(001)$ films with the same composition as shown in Fig. 2(b) at different temperatures (but with the same $^{18}O_2$ pressure [0.01 Torr] and anneal time 30 min) is shown schematically in Fig. 3. The rise of the Si peak area can be directly associated with the SiO_x growth, and will be analyzed separately. The resulting oxygen depth profiles for $Hf_{0.67}Si_{0.33}O_2/SiO_xN_y/Si(001)$ films are shown in Fig. 4. The thickness of the as-deposited silicate layer is marked by a vertical line. The SiO_2/Si system does not have an atomically sharp interface, but changes through a ~5–10 Å thick region.[34] We cannot determine the detailed shape of the oxygen distribution due to straggling effects[27,35] which become severe for buried layers. Silicon suboxide formation and interfacial layer roughness will both contribute to the broadening of the low-energy tail of the ion scattering peaks.[27] As the temperature goes up, the amount of ^{18}O exchanged in Hf silicate layer increases, and so does the depth of ^{18}O incorporation. Oxygen profiles at 973 K show a prominent peak at ~ 45 Å. This is an artifact of the fitting procedure, which assumes that the silicon atomic fraction is constant at 0.33, and therefore the sum of fractions of both oxygen isotopes and nitrogen must be 0.67. Note that since the stoichiometry of the elements in thin films contribute directly to the detected backscattered ion yield, it is a standard assumption in ion beam analysis to keep the sum of the

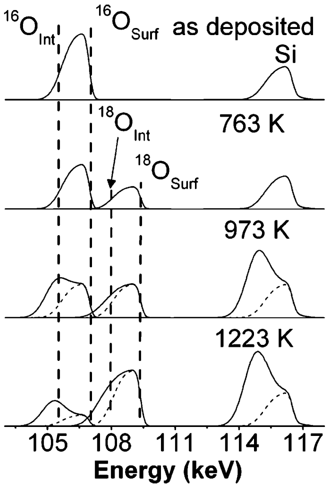

FIG. 3. Schematic representation MEIS spectra for Si, ^{18}O, and ^{16}O energy range of isotopic exchange and incorporation in hafnium silicate film corresponding to (a) as-deposited film, re-oxidized for 30 min at (b) 763 K, (c) 973 K, and (d) 1223 K.

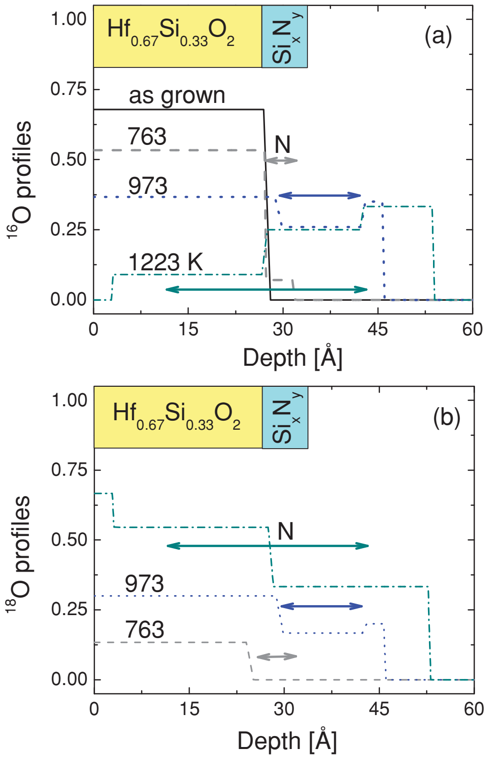

FIG. 4. (Color online) (a) ^{16}O and (b) ^{18}O isotopic depth distributions for hafnium silicate samples oxidized for 30 min at 763–1223 K. Depth distribution profiles are deduced from simulations for the MEIS spectra (schematics of the spectra are shown in Fig. 3). The thickness of the as-deposited silicate layer is marked by a large (yellow) rectangle. The initial $Si_xN_y/Si(001)$ interface position is also shown in the as-deposited samples, whereas horizontal arrows indicate the spread of N during oxidation. Peaks in O profiles for 973 K at ~ 45 Å are due to the fitting constrains which assume Si atomic fraction is constant at 0.33, the sum of fractions of O isotopes and nitrogen must be 0.67. When N content goes to zero at the depth of 42 Å, both O isotopes fractions must go up.

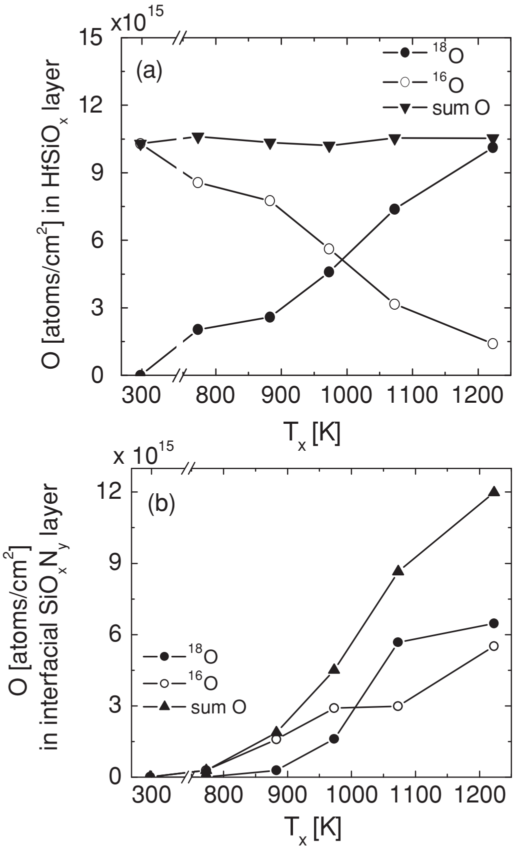

FIG. 5. Variation of oxygen density in (a) hafnium silicate layer and (b) interfacial SiO_xN_y layer is a function of re-oxidation temperature during 30 min anneal at $p_{18O2} = 10^{-2}$Torr.

concentrations of all elements in a given layer as 1 (or at least constant). At 973 K, the nitrogen content goes to zero at a depth of 42 Å, therefore both oxygen isotope fractions must go up. In Fig. 5 we show the ratio of the ^{18}O to ^{16}O content in the Hf-containing layer (the oxygen exchange fraction) as well as in the interfacial SiO_x and SiO_xN_y layer. Two different temperature regimes can be identified. The amount of ^{18}O in the hafnium silicate (exchange fraction) is increasing continuously as the temperature increases. Yet ^{16}O is still the predominant oxygen isotope in the interfacial SiO_x or SiO_xN_y layer at $T \leqslant 973$ K (no net increase, no oxidation of the Si substrate at this temperature, only isotopic exchange). On the other hand, above 1000 K after 30 min annealing the ^{18}O content at the interface is larger than that of ^{16}O. Assuming that the only source of ^{18}O is the gas phase $^{18}O_2$, and ^{16}O is only in the as-deposited films, we can evaluate how much ^{16}O is leaving the samples during this incorporation process. From integrating the area of the ^{16}O peak, we find that we initially have ^{16}O atomic density of 10.3×10^{15} atoms/cm^2 in the as-grown Hf silicate films, and that 6.9×10^{15} atoms/cm^2 remain after the 1223 K annealing in $^{18}O_2$. Therefore ~35% of the ^{16}O atoms have been removed either via an $^{16,18}O_2$ desorption process from the $Hf_{0.67}Si_{0.33}O_2$ surface in direct exchange with gas phase $^{18}O_2$, or via a $Si^{16}O$ desorption from the $SiO_2/Si(001)$ interface. Based on our results, an $^{16,18}O_2$ desorption process is predominant here since SiO desorption from the SiO_2/Si interface would result in a decrease of the SiO_2 layer thickness. However, SiO desorption cannot be excluded completely as a feasible mechanism and it may become import at higher temperatures.[25,36] The remaining ^{16}O is mostly in the interfacial SiO_xN_y layer, as if they have been pushed there by the ^{18}O atoms from the $Hf_{0.67}Si_{0.33}O_2$ layer.

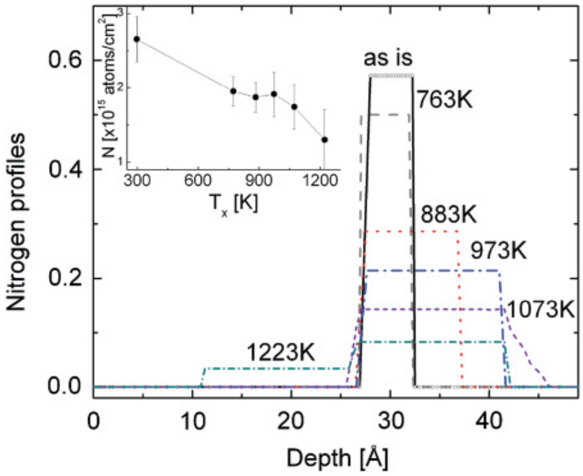

FIG. 6. (Color online) Calculated nitrogen distributions in $Hf_{0.67}Si_{0.33}O_2/SiO_xN_y/Si(001)$ films re-oxidized in $^{18}O_2$ at different temperatures. Fractions of the nitrogen atoms y are shown, with the sum for all the elements adding up to 1. Insert shows integrated nitrogen atom density as a function of re-oxidation temperature.

Selected samples contained nitrogen in the interfacial SiON layer. Therefore we can also compare oxygen isotope distributions and nitrogen depth distributions at various annealing temperatures (Fig. 6), for the same samples as shown in Figs. 4 and 5. The total nitrogen content in these films decreases by approximately a factor of 2 over the temperature range investigated. In addition, the depth distribution broadens quite appreciably. When nitrogen is present, the oxygen distribution extends deeper than the initial nitrogen distribution. The similarity between the areal densities and profiles of incorporated ^{18}O [Fig. 4(b)] and lost N (Fig. 6) suggests an exchange reaction as a principle mechanism responsible for nitrogen loss and oxygen incorporation.

Figure 7 shows an Arrhenius plot of the interface $^{18}O + ^{16}O$ content for three different samples: one with 45 Å of starting SiO_2, another with 45 Å of starting SiO_xN_y, and a third with 27 Å $Hf_{0.67}Si_{0.33}O_2$/6 Å SiO_xN_y, all oxidized in $^{18}O_2$ under similar conditions. In these ultrathin films oxidation is presumably "reaction limited",[37] therefore the interface reaction will be independent of the starting oxide thickness and the increase of ^{18}O at the interface should depend on both time and pressure linearly. One can see that the rate of oxide growth near the interface is almost one order of magnitude lower for the $Hf_{0.67}Si_{0.33}O_2/SiO_xN_y$ films (compared to pure SiO_2). The Arrhenius plots show straight lines with calculated apparent activation energies of 2.7 ± 0.1 eV (SiO_xN_y/Si) (Ref. 26), 3.0 ± 0.1 eV (SiO_2/Si) (Ref. 26), and 0.5 ± 0.1 eV ($Hf_{0.67}Si_{0.33}O_2/Si$). A lower activation barrier value in the case of hafnium-silicate-based films is an indication of a distinctly different oxygen incorporation mechanism.

Oxygen interactions with amorphous and crystalline hafnium oxides and silicates were examined in our earlier

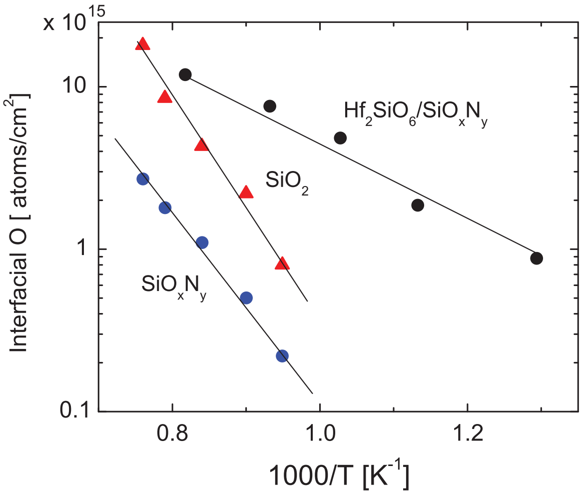

FIG. 7. (Color online) Semilogarithmic dependence of the amount of oxygen atoms incorporated near SiON interface of $Hf_{0.67}Si_{0.33}O_2/SiO_xN_y$ (10^{-2}Torr, 30 min), SiO_xN_y and SiO_2 (7 Torr, 60 min) films on the inverse temperature after re-oxidation in $^{18}O_2$. SiO_xN_y and SiO_2 data are reproduced with permission.

studies.[29] In addition we note here that crystallization anneals of Hf oxide films at 1023 K under UHV conditions results in the development of an additional ~4–5 Å of SiO_2 at the lower (dielectric/Si) interface. In XPS, a comparison of the Si 2*p* peaks for pure HfO_2 films shows that after the 1023 K crystallization anneal, the amount of interfacial SiO_2 increases slightly, consistent with our MEIS observations (Figs. 8 and 9). The origin of this additional interfacial SiO_2 formation will be discussed below.

IV. DISCUSSION

A. Exchange reactions

Our experiments indicated that atomic oxygen diffusion via an oxygen lattice exchange mechanism is the predominant diffusion mechanism in Hf oxide,[29] consistent with theoretical calculations.[19] The *exchange mechanism* involves the continuous replacement of an oxygen lattice site by the diffusing defect (oxygen or vacancy), hence the occupancy and exchange of oxygen in lattice sites is the predominant mode of diffusion. Previous experiments with ZrO_2 films[31] and ultrafine grained ZrO_2 (Ref. 38), and density functional calculations of oxygen incorporation and diffusion energies in monoclinic hafnia (HfO_2) (Ref. 19) have all suggested that oxygen incorporates and diffuses in the atomic (ionic, nonmolecular) form. Furthermore, O^{2-} becomes a more thermodynamically stable interstitial by accepting two electrons.[19] Calculations by the same authors show that diffusion via oxygen lattice exchange should be the favored mechanism, however, the barriers for interstitial oxygen diffusion in HfO_2 are also small, and charged defects could be mobile under high temperature processing conditions. In contrast, molecular oxygen incorporation is preferred for the less-dense SiO_2 structure, with diffusion proceeding through interstitial sites.[39]

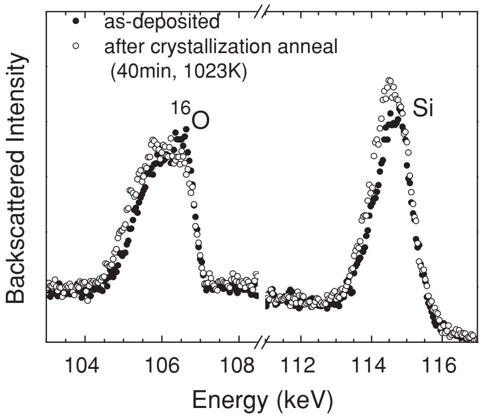

FIG. 8. Si and O peaks in channeling geometry after crystallization anneal of hafnium oxide film in vacuum. Note that the O peak integrated area remains the same, while Si peak increases.

Provided that the transported species are individual oxygen atoms (or ions), the availability of atomic oxygen at the surface is one of the factors affecting the extent of the exchange in the oxide. O_2 is expected to be adsorbed molecularly on perfect surfaces of HfO_2 and to dissociate primarily at O-vacancy defect (or Hf undercoordinated) sites. The amount of available atomic O depends on the rate of O_2 dissociation at the surface, and is therefore related to the number of oxygen vacancies at the top surface. This brings an interesting possibility of blocking oxygen dissociation by adsorption of a monolayer of SiO_2. The covalent bonding of this layer will inhibit oxygen dissociation, and therefore inhibits its further diffusion and the interfacial SiO_2 growth. Additionally, as the structural heterogeneity of atoms along the diffusion path may facilitate the lattice exchange of oxygen, as-deposited disordered HfO_2 films might be expected to display a lower diffusion barrier than crystalline films.

We note that the kinetics of oxygen exchange (Fig. 2) may be controlled to a large extent by crystallization of the as-deposited film occurring in parallel with the exchange. An onset of amorphous Hf oxide crystallization was reported at a temperature as low as 723–773 K, resulting in the formation of a monoclinic phase;[22] whereas Hf silicate is stable with respect to phase segregation at these temperatures. During

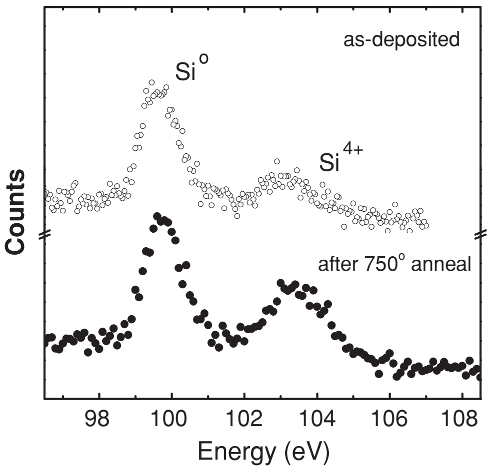

FIG. 9. XPS data for the Si 2*p* region from $HfO_2/SiO_2/Si(001)$ (normalized to the Si° peak).

annealing at $T \geqslant 1073$ K Hf silicate films are reported to phase separate into a crystalline HfO_2-rich phase imbedded in an amorphous silica-rich matrix.[40] Moreover, phase separation in Hf silicates is complex and remains controversial. Some authors have argued that it can proceed by nucleation and growth, or by spinodal decomposition mechanisms dependent on composition and temperature ranges, resulting in different microstructures.[41,42] There have been no reports of phase separation in the temperature, composition, and thickness ranges explored in Fig. 2: (773 K)/ ($Hf_{0.67}Si_{0.33}O_2$)/(27 Å). While the exchange process is fast for Hf oxide in the first few minutes, it slows down (or stops at a significantly long annealing time (∼120 min). Considering that (a) $^{18}O_2$ is in excess in the gas phase (10^{-2} Torr), (b) the amount of ^{16}O is limited and well known in as-deposited Hf oxide films, and (c) ∼50% of ^{16}O atoms were exchanged by ^{18}O in the first 30 min (see Table I), one can then expect that >75–80% of oxygen atoms within the Hf oxide framework should be ^{18}O atoms under the conditions listed above. However, this is not the case: ^{18}O atoms constitute only ∼55% of the total oxygen content after 120 min of annealing at 763 K [Fig. 2(c). We speculate that during longer oxidation anneals, when crystallization is completed and most of the available oxygen dissociation centers at the oxide surface are blocked by bonded oxygen atoms, diffusion and exchange would proceed predominantly via molecular oxygen incorporation and diffusion via grain boundaries, therefore slowing down the extent of exchange significantly.

The incorporation of nitrogen is a well known way to reduce diffusion of certain elements (e.g., boron, arsenic, and phosphorous diffusion is decreased when nitrogen is incorporated in SiON dielectric layers).[43,44] In our work, nitrogen incorporation into the network of the Hf silicates does not change the exchange fraction of oxygen significantly, if only oxygen atoms are considered in the diffusion process. Therefore the main action of nitrogen is in the reduction of reactive sites for the active species, such as O; the remaining Hf-O-Hf framework will be as active in the oxygen exchange process as it would be in the absence of incorporated nitrogen. Ultimately nitrogen incorporation into the Hf-Si-O network to form HfSiON promotes phase stability and improves electrical performance.[45] Morais *et al.* showed in x-ray absorption near edge structure (XANES) that while Hf silicate forms a $(HfO_2)_{1-x}(SiO_2)_x$ pseudobinary alloy upon annealing, while the $Hf_{1-x}Si_xO_{2-n}N_n$ system remains amorphous after the 1275 K, 60 s anneal.[45] Since one of the possible diffusion routes for dopant elements is via grain boundaries, nitrogen incorporation suppresses grain boundary formation during phase segregation and thus dopant diffusion is reduced significantly.[46]

B. Growth of the interfacial silicon oxide layer

The thermodynamics of SiO_x layer growth at the interface is controlled by the migration of oxygen toward the Si substrate. The rate limiting step in HfO_2/Si interface oxidation appears to be O_2 going from the gas phase into the HfO_2 lattice, while in the SiO_2/Si case, the rate limiting step appears to be interstitial O_2 dissociation and insertion at the SiO_2/Si interface. Once oxygen incorporates at the HfO_2/Si interface, forming an HfO_2/SiO_2/Si structure, the oxidation rate decreases significantly. The key energy for the oxidation process is the total energy for moving an oxygen molecule from the gas phase into an interstitial site in the Hf oxide (silicate) in comparison to the insertion energy for the SiO_2/Si case. Our results indicate that the insertion energy is much lower for the former case.

When interstitial oxygen gets to the $HfSiO_x/SiO_2$ interface, at low temperatures (<1000 K) it is likely to incorporate in the Si-O-Si framework forming the Si-O-O-Si-peroxy linkages as in the SiO_2 case.[27,47,48] At higher temperatures (>1000 K) additional channels open up for the molecular oxygen to migrate through the grain boundary (or through the more open Si-O-Si network in the case of the Hf silicate) to bring molecular $^{18}O_2$ to the interface for direct oxidation.[49] This is why (see Fig. 7) we suggest there is an increase of ^{18}O in the interfacial SiO_x layer compared to the exchange (in $HfSiO_x$) fraction above 1000 K.

With regard to interfacial oxide growth, the presence of an interfacial silicon nitride layer modifies the ^{18}O-^{16}O into ^{18}O-N exchange, which slows diffusion and reduces the oxidation rate. When nitrogen is present in the interfacial SiO_xN_y layer, additional SiO_2 layer growth occurs primarily below the SiON layer. Hence there is a relatively slow ^{18}O-N displacement exchange in the SiO_xN_y layer. Gavartin *et al.*[50] found that nitrogen anneals of high-κ dielectric oxides lead to the relative immobilization of defects such as oxygen vacancies and interstitial oxygen ions. In addition to the positive defect passivation benefits of incorporating N in the Si/high-κ (SiO_x) interface layer, high N concentrations near the Si substrate interface have been shown to compromise other aspects of device performance and reliability. Our findings illustrate that, although the N depth distribution profile broadens during high temperature annealing in ^{18}O, N is displaced from the Si substrate during the interfacial SiO_xN_y growth process. This demonstration suggests that the accurate control of the Si substrate oxidation may be an effective means of tuning the N concentration profile with respect to the substrate for performance enhancement. Finally, we note that interface growth can result from internal oxygen sources (oxygen trapped in the film during film deposition) as well as external ones. The effect of postdeposition annealing on HfO_2 film composition and HfO_2/Si interfacial structure clearly shows that SiO_2 starts to develop at the interface as the annealing temperature is raised to 773 K *without oxygen in the gas phase*. Therefore we conclude that there are at least two possible oxygen sources for interfacial SiO_2 growth. In addition to relatively slow interfacial growth caused by excess oxygen in the gas phase (external source), for ALD grown high-κ films intrinsic fast sources for interfacial oxide growth may exist, such as overstoichiometric oxygen trapped as, for instance, -OH in the dielectric layer (internal source).[7,51]

V. CONCLUSION

High-resolution ion scattering with isotopic tracing was used to examine oxygen exchange and the mechanism of interfacial growth in hafnium-based ultrathin dielectric films. The complex oxidation behavior is likely to be a combination of interfacial, near-interfacial, and surface reactions. HfO_2/SiO_2/Si(001) samples exposed to ^{18}O at low temperatures exhibit mostly oxygen exchange (^{16}O for ^{18}O) in the overlayer with no net interfacial oxide growth. The same exposure of the hafnium silicate films also exhibits only isotopic oxygen exchange (no net oxide growth) albeit at a significantly reduced rate, owing to the presence of amorphous HfSiON compared with the grain-boundary-assisted diffusion rate associated with the crystalline HfO_2 sample. Exposure of the Hf silicate film system to ^{18}O at higher temperatures results in a much higher ^{18}O/^{16}O exchange rate throughout the Hf silicate film. Concurrent with the exchange, interfacial SiO_xN_y is grown due to the supply of the displaced ^{16}O (as well as ^{18}O) that migrates toward the Si substrate; both oxygen isotopes are present at the interface in near-equal abundance. Our findings suggest that an oxidation anneal process may be developed to accurately control the N profile proximity to the Si substrate for performance enhancement.

ACKNOWLEDGMENTS

The work at Rutgers was supported by NSF Grant No. DMR-0706326. We also thank the SRC/Sematech FEP-TC and CAPES (Brazil) for financial support.

---

[*] Present address: Department of Physics and Astronomy, University of Western Ontario, London, Canada ON N6A 3K7.

[1] D. G. Schlom, S. Guha, and S. Datta, MRS Bull. **33**, 1017 (2008).

[2] M. M. Frank, S. Kim, S. L. Brown, J. Bruley, M. Copel, M. Hopstaken, M. Chudzik, and V. Narayanan, Microelectr. Eng. **86**, 1603 (2009).

[3] A. A. Demkov and A. Navrotsky, *Materials Fundamentals of Gate Dielectrics* (Springer, Dordrecht, 2005).

[4] J. J. Peterson, C. D. Young, J. Barnett, S. Gopalan, J. Gutt, C.-H. Lee, H.-J. Li, T.-H. Hou, Y. Kim, C. Lim, N. Chaudbary, N. Moumen, B.-H. Lee, G. Bersuker, G. A. Brown, P. M. Zeitzoff, M. I. Gardner, R. W. Murto, H. R. Huff, Electrochem. Solid State Lett. **7**, G164 (2004).

[5] J. K. Schaeffer, L. R. C. Fonseca, S. B. Samavedam, Y. Liang, P. J. Tobin, and B. E. White, Appl. Phys. Lett. **85**, 1826 (2004).

[6] M. Copel, Appl. Phys. Lett. **92**, 152909 (2008).

[7] Y. Wang, M.-T. Ho, L. V. Goncharova, L. S. Wielunski, S. Rivillon-Amy, Y. J. Chabal, T. Gustafsson, N. Moumen, and M. Boleslawski, Chem. Mater. **19**, 3127 (2007).

[8] N. Goel, W. Tsai, C. M. Garner, Y. Sun, P. Pianetta, M. Warusawithana, D. G. Schlom, H. Wen, C. Gaspe, J. C. Keay, M. B. Santos, L. V. Goncharova, E. Garfunkel, and T. Gustafsson, Appl. Phys. Lett. **91**, 113515 (2007).

[9] L. V. Goncharova, M. Dalponte, T. Gustafsson, O. Celik, E. Garfunkel, P. S. Lysaght, and G. Bersuker, J. Vacuum Sci. Technol. A **25**, 261 (2007).

[10] H. Kim, P. C. McIntyre, C. O. Chui, C. Saraswat, and S. Stemmer, J. Appl. Phys. **96**, 3467 (2004).

[11] R. J. Carter, E. Cartier, A. Kerber, L. Pantisano, T. Schram, S. De Gendt, and M. Heyns, Appl. Phys. Lett. **83**, 533 (2003).

[12] J. C. Hackley, T. Gougousi, and J. D. Demaree, J. Appl. Phys. **102**, 034101 (2007).

[13] M. P. Agustin, G. B. Bersuker, B. Foran, L. A. Boatner, and S. Stemmer, J.Appl.Phys. **100**, 024103 (2006).

[14] S. Stemmer, J. Vac. Sci. Technol. B **22**, 791 (2004).

[15] R. M. C. de Ameida and I. J. R. Baumvol, Surf. Sci. Reports **49**, 1 (2003).

[16] We define oxygen exchange as the substitution of the oxygen atoms within the framework of the thin film by oxygen coming from the gas phase. The number of atoms gained from the gas phase is equal to the number of oxygen atoms lost, so the total oxygen content of the dielectric remains constant during the exchange. This exchange process has to be differentiated from interfacial incorporation and growth, where oxygen reacts with the film or the substrate, increasing the total oxygen content.

[17] H. S. Baik, M. Kim, G.-S. Park, S. A. Song, M. Varela, A. Franceschetti, S. T. Pantelides, and S. J. Pennycook, Appl. Phys. Lett. **85**, 672 (2004).

[18] J. X. Zheng, G. Ceder, T. Maxisch, W. K. Chim, and W. K. Choi, Phys. Rev. B **75**, 104112 (2007).

[19] A. S. Foster, A. L. Shluger, and R. M. Nieminen, Phys. Rev. Lett. **89**, 225901 (2002).

[20] D. Ceresoli and D. Vanderbilt, Phys. Rev. B **74**, 125108 (2006).

[21] C. Tang and R. Ramprasad, Phys. Rev. B **81**, 161201 (2010).

[22] S. V. Ushakov, C.E. Brown, A. Navrotsky, A.A. Demkov, C. Wang, and B.-Y. Nguyen, Phys. Stat. Sol. B **241**, 2268 (2004).

[23] J. Liu, W. N. Lennard, L. V. Goncharova, D. Landheer, X. Wu, S. Rushworth, and A. C. Jones, J. Electrochem. Soc. **156**, G89 (2009).

[24] K. Taniguchi, Y. Shibata, and C. Hamaguchi, J. Appl. Phys. **65**, 2723 (1989).

[25] I. C. Vickridge, O. Kaitasov, R. J. Chater, and J. A. Kilner, Nucl. Instrum. Meth. B **161–163**, 441 (2000).

[26] H. C. Lu, Ph.D. thesis, Rutgers University, 1997.

[27] E. P. Gusev, H. C. Lu, T. Gustafsson, and E. Garfunkel, Phys. Rev. B **52**, 1759 (1995).

[28] H. C. Lu, E. P. Gusev, E. Garfunkel, B. W. Busch, T. Gustafsson, T. W. Sorsch, and M. L. Green, J. Appl. Phys. **87**, 1550 (2000).

[29] L. V. Goncharova, M. Dalponte, T. Gustafsson, E. Garfunkel, P. S. Lysaght, B. Foran, J. Barnett, and G. I. Bersuker, Appl. Phys. Lett. **89**, 044108 (2006).

[30] R. M. Tromp, M. Copel, M. C. Reuter, M. Horn von Hoegen, J. Speidell, and R. Koudijs, Rev. Sci. Instrum. **62**, 2679 (1991).

[31] B. W. Busch, W. H. Schulte, E. Garfunkel, T. Gustafsson, W. Qi, R. Nieh, and J. Lee, Phys. Rev. B **62**, R13 290 (2000).

[32] T. Nishimura, *MEIS simulation program*, v. 1.02, 2005 (personal communication).

[33] W. H. Schulte, B. W. Busch, E. Garfunkel, T. Gustafsson, G. Schiwietz, and P. L. Grande, Nucl. Instrum. Meth. B **183**, 16 (2001).

[34] An estimate of the error of the width of this region is ~ 5 Å; taking into account an additional shift of 2 Å from the asymmetry of energy straggling, we have an $\sim 13 \pm 5$ Å thick transition region, where the oxide structure deviates from the amorphous SiO_2

[35] N. Bohr and K. Dan, Selsk. Mat. Fys. Medd. **18**, 8 (1948).

[36] I. J. R. Baumvol, C. Krug, F. Stedile, F. Gorris, and W. H. Schulte, Phys. Rev. B **60**, 1492 (1999).

[37] P. Atkins, *Physical Chemistry* (Freeman, New York, 1998).

[38] U. Brossmann, R. Wurschum, U. Sodervall, and H. Schaefer, J. Appl. Phys. **85**, 7646 (1999).

[39] S. Mukhopadhyay, P. V. Sushko, A. M. Stoneham, and A. L. Shluger, Phys. Rev. B **71**, 235204 (2005).

[40] D. A. Neumayer and E. Cartier, J. Appl. Phys. **90**, 1801 (2001).

[41] S. Stemmer, Y. L. Li, B. Foran, P. Lysaght, S. K. Streiffer, P. Fuoss, and S. Seifert, Appl. Phys. Lett. **83**, 3141 (2003).

[42] J. Liu, X. Wu, W. N. Lennard, and D. Landheer, Phys. Rev. B **80**, 041403 (2009).

[43] E. P. Gusev, H. C. Lu, E. Garfunkel, T. Gustafsson, M. L. Green, D. Brasen, and W. N. Lennard, J. Appl. Phys. **84**, 2980 (1998).

[44] M. Quevedo-Lopez, M. El-Bouanani, M. J. Kim, B. E. Gnade, R. M. Wallace, M. R. Visokay, A. Li-Fatou, M. J. Bevan, and L. Colombo, Appl. Phys. Lett. **81**, 1609 (2002).

[45] J. Morais, L. Miotti, K. P. Bastos, S. R. Teixeira, I. J. R. Baumvol, A. L. P. Rotondaro, J. J. Chambers, M. R. Visokay, L. Colombo, and M. C. Martins Alves, Appl. Phys. Lett. **86**, 212906 (2005).

[46] C. Driemeier, K. P. Bastos, G. V. Soares, L. Miotti, R. P. Pezzi, I. J. R. Baumvol, P. Punchaipetch, G. Pant, B. E. Gnade, and R. M. Wallace, Appl. Physics A **80**, 1045 (2005).

[47] A. M. Stoneham, M. A. Szymanski, and A. L. Shluger, Phys. Rev. B **63**, 241304 (2001).

[48] M. A. Szymanski, A. L. Shluger, and A. M. Stoneham, Phys. Rev. B **63**, 224207 (2001).

[49] A. M. Stoneham, J. L. Gavartin, and A. L. Shluger, J. Phys.: Condens. Matter **17**, S2027 (2005).

[50] J. L. Gavartin, A. L. Shluger, A. S. Foster, and G. Bersuker, J. Appl. Phys. **97**, 053704 (2005).

[51] M.-T. Ho, Y. Wang, R. T. Brewer, L. S. Wielunski, Y. J. Chabal, N. Moumen, and M. Boleslawski, Appl. Phys. Lett. **87**, 133103 (2005).